

Article

Numerical Simulation on Smoke Temperature Distribution in a Large Indoor Pedestrian Street Fire

Weidong Lin ¹, Qiyu Liu ², Meihong Zhang ³, Bihe Cai ⁴, Hui Wang ⁵, Jian Chen ⁶ and Yang Zhou ^{2,*}¹ Fujian Provincial Institute of Architectural Design and Research Co., Ltd., Fuzhou 350001, China² School of Civil Engineering, Central South University, Changsha 410075, China³ Xiamen Fire Rescue Detachment, Xiamen 361013, China⁴ YanGuo Technology Co., Ltd., Xiamen 361001, China⁵ Fujian Construction Engineering Group Co., Ltd., Fuzhou 350001, China⁶ China Academy of Building Research, Beijing 100013, China

* Correspondence: zyzhou@csu.edu.cn

Abstract: In order to study the characteristics of fire smoke spread and temperature distribution of a large indoor pedestrian street under different heat release rates and smoke exhaust modes, this paper focuses on the analysis of fire smoke spread, visibility, smoke temperature distribution and variation curves in an atrium. This paper uses a numerical simulation method to conduct research. PyroSim fire simulation software is used to calculate this project, which is based on a full-scale experimental design scheme. The numerical simulation results show that under the conditions of higher heat release rate, the smoke spread rate is greater than that under the conditions of lower heat release rate. Furthermore, the average temperature of smoke in the atrium is also greater, up to about 400 °C. The conditions of a higher heat release rate also show the characteristics of faster generation, faster spread and a larger volume of smoke. When the smoke exhaust system is turned on, the thickness of the smoke layer and the smoke temperature decrease. There then comes a situation where the stable section of the fire ends in advance. The simulation results of vertical temperature distribution in an atrium can fit the modified McCaffrey plume model in any case. Under all cases, the smoke temperature reaches the maximum directly above the fire source. The horizontal dimensionless smoke temperature rises under the atrium roof, and decreases exponentially with the dimensionless distance from the fire source. The greater the heat release rate of fire source is, the smaller the attenuation coefficient is, with a more than 50% change. When the smoke exhaust system is turned on, the smoke flow accelerates and the smoke is cooled rapidly. Thus, the attenuation coefficient increases. Additionally, the effect of mechanical smoke exhaust is better than natural smoke exhaust, because mechanical smoke exhaust makes air flow and heat exchange more intense. The variation amplitudes of the attenuation coefficient under natural smoke exhaust and mechanical smoke exhaust are 13% and 22%, respectively.

Keywords: safety engineering; numerical simulation; large indoor pedestrian street fire; smoke spread; temperature distribution; smoke exhaust



Citation: Lin, W.; Liu, Q.; Zhang, M.; Cai, B.; Wang, H.; Chen, J.; Zhou, Y. Numerical Simulation on Smoke Temperature Distribution in a Large Indoor Pedestrian Street Fire. *Fire* **2023**, *6*, 115. <https://doi.org/10.3390/fire6030115>

Academic Editor: Dahai Qi

Received: 3 February 2023

Revised: 3 March 2023

Accepted: 7 March 2023

Published: 13 March 2023



Copyright: © 2023 by the authors. Licensee MDPI, Basel, Switzerland. This article is an open access article distributed under the terms and conditions of the Creative Commons Attribution (CC BY) license (<https://creativecommons.org/licenses/by/4.0/>).

1. Introduction

With the rapid development of the social economy and the advancement of modernization, urban economies have gradually developed in the direction of diversification to meet the growing needs of people for a better life. Thus, a large number of urban commercial complexes have emerged. These commercial complexes integrate entertainment, catering, fitness, shopping, offices and other functions, which greatly meet the needs of life, and bring much comfort and convenience. Indoor pedestrian streets are commonly found in various complexes and are one of their core architectural elements, found in various forms, and also in different lengths and heights. Due to the unique narrow and long building structure of the indoor pedestrian street, and the large number of combustibles in it coupled with

the dense population and high mobility, once a fire occurs, the fire is very likely to spread to the atrium. It will spread further into the adjacent buildings through the pedestrian street walkway, causing irreparable losses. On 15 February 2004, a particularly serious fire accident occurred in Zhongbai Commercial Building in Jilin, Jilin Province. The fire was caused by the fire of a warehouse built nearby the commercial building which then spread to it. The evacuation exit was blocked, resulting in 54 deaths and more than 70 injuries. On 30 June 2012, a major fire accident occurred in the Ryde Commercial Building in Jixian, Tianjin, resulting in 10 deaths and 16 serious injuries, which was caused by electrical sparks due to overloaded air conditioning. In recent years, fire accidents in shopping malls and pedestrian streets are emerging one after another, and their serious fire risks have attracted great attention from society. Therefore, it is an obligation to research the laws of smoke spread and temperature distribution in atriums and indoor pedestrian streets, to conduct the decisive factor for personnel safety evacuation [1,2].

The spread of smoke in pedestrian streets and large atriums, the laws of temperature distribution and the effect of smoke exhaust systems have always been the focus of research of many scholars at home and abroad. Hu et al. [3] obtained the characteristics of smoke spread and the temperature distribution law of fire below the ceiling by conducting full-scale fire experiments in a long walkway. Huo [4] and others conducted fire experiments in a large-space fire experimental hall, and preliminarily studied the mechanical smoke extraction efficiency of large-space building fires. The full-scale experiment can realistically reproduce the fire scene and achieve a high degree of matching with real fire, which is very reliable. However, because of many large experimental scenes, the experiment is quite difficult, being both laborious and time-consuming. Thus, the limitations of full-scale experiments are reflected. In recent years, CFD numerical simulation technology has matured and improved, bringing not only good visualization effects, but also high fidelity, in addition to including many parameters that cannot be measured by experiments. The technology has gradually become the mainstream research method for studying large-space fires. Rho [5] and Mowrer et al. [6] used numerical simulation technology to study the smoke spread characteristics of a fire in a large-space atrium. Hadjisophocleous et al. [7] combined solid experiments and numerical simulation to analyze the smoke spread characteristics of atrium fires and the calculation method of smoke layer height. Long et al. [8] carried out full-scale fire experiments to investigate some key parameters, including the vertical and longitudinal temperature distribution, smoke layer height and smoke front arrival time under four different cases. In Jiao's work, a series of full-scale fire tests were performed to study the smoke spread characteristics and temperature distribution of indoor pedestrian street fires with different mechanical smoke exhaust modes [9]. Tian and Cai [10] used FDS to analyze and evaluate the fire hazard, effectiveness of smoke prevention measures and personnel safety of commercial complexes, and proposed performance-based design solutions. Zhao [11] studied the law of fire smoke spread and the control mode and effect of smoke in buildings through FDS numerical simulation technology, and obtained the influence of different smoke exhaust positions, fire source power, floor opening rate, smoke trapping wall height, etc., on smoke spread and the effects of smoke extraction. Jiang [12] used Fluent software to study the influence of the position of the air outlet on the smoke flow and smoke extraction effect of the atrium space of the mall, and proposed an optimization scheme.

It can be seen from the research status at home and abroad that the research on smoke control theory and smoke extraction mode has been relatively detailed. Although many studies have been carried out on large-space indoor pedestrian street fires, most of them focus on the influence of different smoke exhaust locations or smoke control modes on the flow and control of fire smoke. There are few studies on the temperature distribution characteristics of fire smoke in large-space indoor pedestrian streets. Therefore, this paper aims to study and discuss the characteristics of atrium smoke spread, vertical smoke temperature distribution and horizontal smoke temperature distribution under the ceiling

under different ignition heat release rates, and establish a dimensionless theoretical model of smoke temperature rise.

2. Numerical Simulation Parameter Setting and Experimental Verification

2.1. Introduction of PyroSim

Fire numerical simulation research technology began in the 1960s. Over decades of continuous development and breakthrough, relatively mature research methods have been formed. Currently, fire numerical simulation research has been widely used in building fire research, performance building fire design, personnel safety escape and evacuation and other aspects. In this paper, PyroSim simulation software was selected to study the fire characteristics of indoor pedestrian streets for numerical simulation. This software is a fire dynamic simulation software based on the principle of large eddy simulation (LES), researched and developed by the National Institute of Standards and Technology (NIST). PyroSim is based on computational fluid dynamics and provides fire simulation parameters and fire model settings with a visual interface, which can accurately simulate and predict fire smoke spread, temperature, visibility, toxic and harmful gas concentration distribution and other parameter indicators [13,14].

2.2. Commercial Pedestrian Street Experiment

The experimental area was located in a pedestrian street and adjacent ring corridor in a building complex in Fuzhou, as shown in Figure 1. The building has 4 floors, each with a floor height of 4.5 m, and the pedestrian street is a narrow and straight, 154 m long and 17 m wide. Corridors on both sides are 4 m wide with a height of 2.8 m under the ceiling. The pedestrian street contains three atriums 1#, 2# and 3#. All three atriums are 19.8 m high. The experimental location is Atrium 2#, which is 32.4 m long and 8 m wide. The doors and windows on both sides of the ring corridor were kept closed during the experiment. The smoke exhaust system was opened according to different working conditions of the experiment, and the volume of the top smoke exhaust fan was 64,200 m³/h.

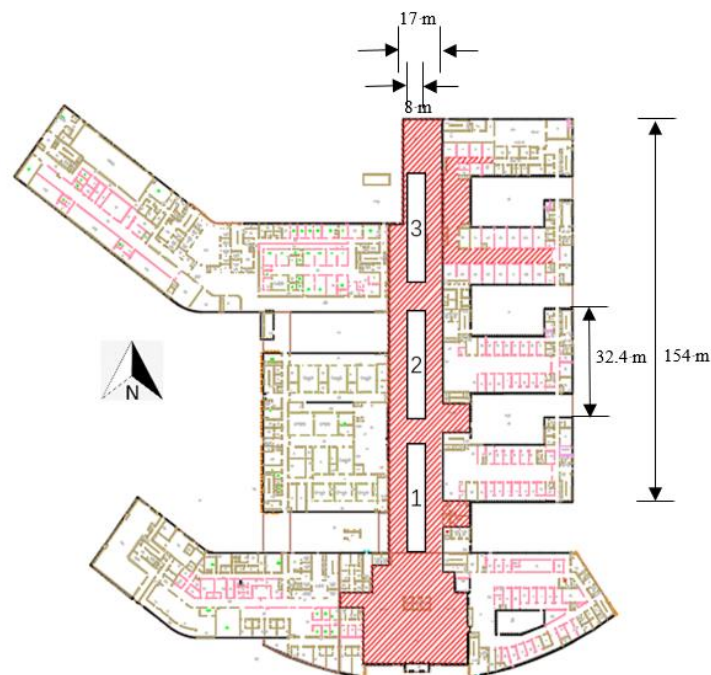


Figure 1. Plan of a building complex in Fuzhou.

The experimental working conditions include natural filling, natural smoke exhaust and atrium mechanical smoke exhaust. Specific working conditions are detailed in Table 1.

Table 1. Experiments' conditions.

Case	Heat Release Rates	Fire Location	Smoke Exhaust Mode
Case 1	1.5 MW	Atrium 2#	natural filling
Case 2	1.5 MW	Atrium 2#	natural smoke exhaust
Case 3	0.7 MW	Atrium 2#	natural filling
Case 4	0.34 MW	Atrium 2#	natural smoke exhaust
Case 5	0.34 MW	Atrium 2#	mechanical smoke exhaust

During the experiment, the fire source was arranged in the center of atrium 2#, as shown in Figure 2 in accordance with the requirements of the standard hot smoke test method [15] specified in the 'Field Verification Method for the Performance of the Anti-smoke System' (GA/T 999-2012). The designed heat release rates are 1.5 MW, 0.7 MW and 0.34 MW.

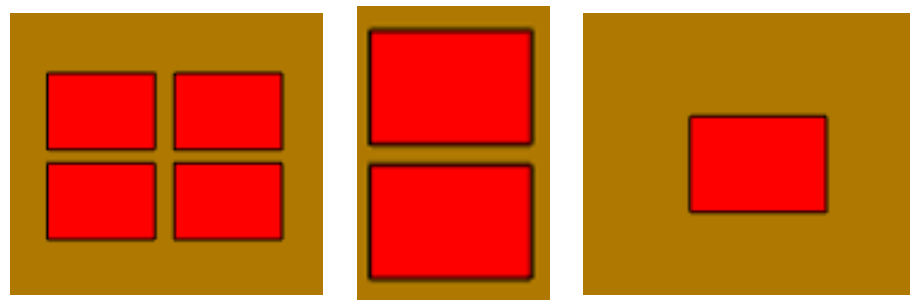


Figure 2. Schematic diagram of fire source layout of different heat release rates (1.5 MW, 0.7 MW, 0.34 MW, from left to right).

The basic components of the whole set of devices include the combustion plate placed in the water tray and the smoke generating device close to the combustion plate. The heat generated by the combustion of the fire source drives the tracer smoke movement to simulate the smoke spread behavior under the real fire. The combustion disc in the hot smoke test device was welded from 1.6 mm thick steel plate, and the internal dimensions were 841 mm × 595 mm × 130 mm. The plate area was 0.5 m², 95% ethanol was selected as fuel, 16 L was injected for each test. Cooling water was injected into the water-bearing plate to ensure the test safety, and the combustion plate will not float. Ammonium chloride smoke cake was selected as the smoke generating material for the test. The smoke generated by combustion was guided to the top of the fire source through an independent smoke generator. The tracer smoke was neutral, white, and basically free of residue.

Five thermocouples were arranged directly above the fire source. The bottom thermocouple was 0.9 m away from the fire source, and the next ones were arranged every next 0.35 m upward, numbering 1~5 in order. The top thermocouple was 2.3 m away from the fire. From the No. 5 thermocouple, they then diverged to the south, east, north and west directions, and along that axis, 2 thermocouples were arranged in each direction at intervals of 0.35 m, numbered 6~13 in turn. There were 13 thermocouples in total.

A thermocouple was arranged every 1 m at 2.3 m from the fire source. The highest point was 17.3 m, and they were numbered V1~V16 from top to bottom, to a total of 16 thermocouples. 7 thermocouples were arranged along the center line from west to east at the height of 9.3 m, 13.8 m and 18.3 m. The horizontal distance interval was 1 m. thermocouples were numbered Z3F1~Z3F7, Z4F1~Z4F7, ZTH1~ZTH7 from west to east in order, to a total of 21. A total of 37 thermocouples were used in this experiment. See Figure 3 for thermocouple layout.

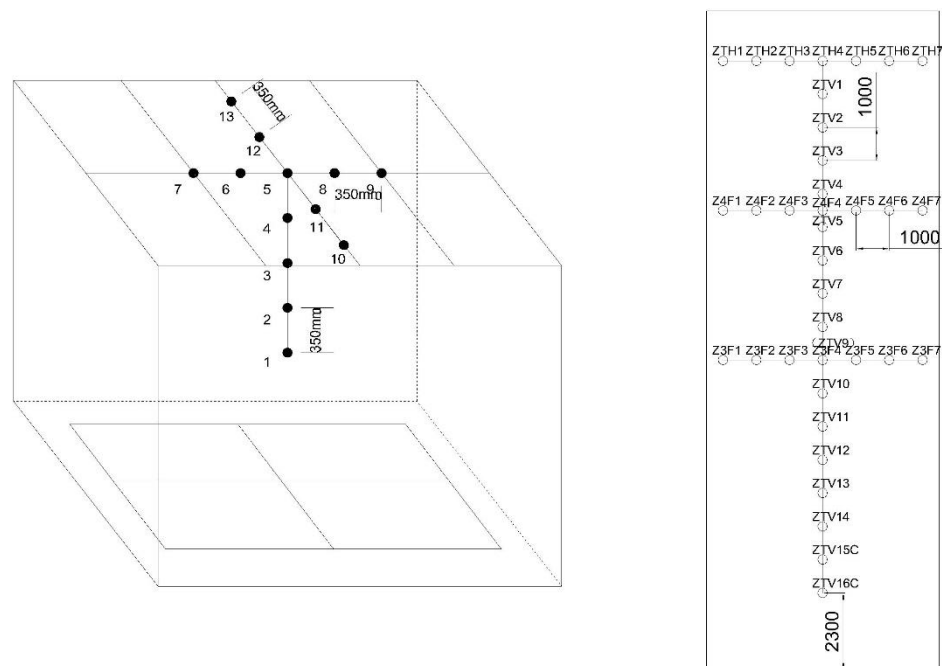


Figure 3. Thermocouple layout.

2.3. Model Parameter Setting

According to the building entity, a numerical model was established according to the size of 1:1. The wall material is made of concrete material and glass curtain wall, and all details of the model are consistent with the actual situation. The corresponding measurement points were set at each place of the thermocouples determined in the laboratory, and the temperature slices are placed in the X and Y directions at the center point of the fire source. The design heat release rates are 1.5 MW, 0.7 MW and 0.34 MW. The fire model is a t^2 fast fire. The simulated initial temperature was 20 °C. The simulation time was consistent with the experimental time, and all doors and windows were kept closed.

The smoke exhaust vents were set in the smoke storage bin on the roof of the building and consisted of 52 vents. A total of 20 natural smoke exhaust vents with lengths of 1.5 m and heights of 0.4 m were set on the east and west sides. Furthermore, 6 mechanical smoke exhaust vents with lengths of 1.2 m and heights of 0.4 m were set on the north and south sides.

During the series of tests, the start-up time of the mechanical smoke exhaust system was 30 s after ignition, and the ambient temperature was always maintained at about 20 °C. The next group of tests were conducted after the environmental conditions recovered to the initial state.

The schematic diagram of numerical model of this complex is shown in Figure 4.

2.4. Grid Independence Analysis

When FDS is used for fire simulation, the mesh size has a greater impact on the experimental results. The smaller the mesh size, the smaller the numerical fluctuation of the simulation results, the more accurate the experimental results, and the longer the simulation time. Thus, it is very important to select the appropriate mesh size for fire simulation. The dimensionless expression $D^* = \delta_x$ is given in the FDS Operation Manual [16], and δ_x is the nominal size of the grid cell. Its definition formula is as follows:

$$D^* = \left[\frac{Q}{\rho_0 c_p T_0 \sqrt{g}} \right]^{2/5} \tag{1}$$

where D^* is the characteristic diameter of fire, m; Q is the heat release rate, kW; g is the acceleration of gravity, m/s^2 ; ρ_0 is the ambient air density, $1.29 \text{ kg}/m^3$; c_p is the specific heat capacity at constant pressure, $1.005 \text{ kJ}/(\text{kg}\cdot\text{K})$; T_0 is the ambient air temperature, 293 K. Taking the heat release rate of 1.5 MW as an example, the characteristic size of the fire is $D^* = 1.09 \text{ m}$. It is generally believed that when the ratio of characteristic diameter to grid is 4~16, the simulation results are more accurate, that is, the grid size is 0.27~0.06 m. Due to the large volume of the physical model, the grid size of the atrium is assumed to be 0.3 m, which basically meets the operation conditions.



Figure 4. Schematic diagram of numerical model of a building complex.

2.5. Experimental Verification of Numerical Simulation Results

As is can be seen from Figure 5, under the same working conditions, the experimental results are in good agreement with the numerical simulation results. However, the experimental temperature data will drop sharply at a certain moment. Through observing the experimental video, we know that the phenomenon is caused by the phenomenon of flame fusion and separation during the experiment, so that the temperature data of the measurement point in the center will fluctuate greatly, which is a normal phenomenon. From the overall temperature change trend, this effect can be ignored, and the data error is within an acceptable range. Therefore, we believe that the calculation results of the numerical simulations in this paper are trustworthy.

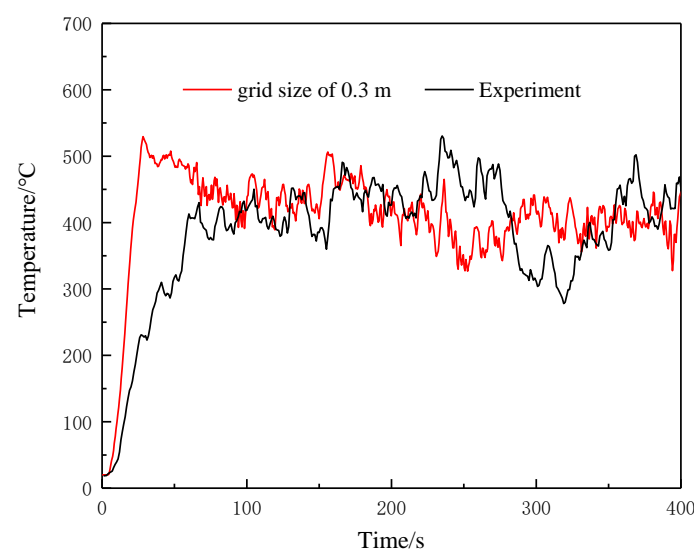


Figure 5. Comparison of temperature change between experiment and numerical simulation of measuring point 1 in Case 1.

Analyzing the two sets of data of numerical simulations and experiments for variance, the sum of three squared errors was calculated to construct the test statistic: $SSA = \sum_{i=1}^r \sum_{j=1}^n (\bar{x}_i - \bar{\bar{x}})^2$, $SSE = \sum_{i=1}^r \sum_{j=1}^n (\bar{x}_{ij} - \bar{x}_i)^2$. The total deviation squared sum $SST = SSA + SSE$, and the corresponding degrees of freedom are $r - 1, n - r, n - 1$, thus determining the mean square MSA, MSE and MST between groups. The required test statistics F can be obtained by the ratio of MSA and MSE, $F = MSA/MSE$. Based on significance level α , compare F and $F_{\alpha}(r - 1, n - r)$ [17]. The calculation results of analysis of variance are shown in Table 2.

Table 2. Calculation results of analysis of variance.

Error Source	Sum of Squares	Freedom	Mean Square	F	$F_{\alpha}(r - 1, n - r)$
Intergroup differences	2.08291×10^6	1	2.08291×10^6	113.26094	3.85
Intragroup differences	2.21971×10^7	1027	18390.333		
Sum	2.428×10^7	1028			

By calculation, it can be seen that at the significance level of 0.05, F is significantly greater than F_{α} , showing a significant difference between the two sets of data.

3. Analysis and Discussion of Numerical Simulation Results

3.1. Analysis of Smoke Spread in Atrium Fire

A large amount of smoke and heat generated during a fire will form a hot smoke stream. The flow direction of the smoke is often the direction of the fire spread, and the flow speed of the smoke is often the fire spreading speed [18]. The smoke will gradually collect over the atrium, and the smoke layer will continue to settle, which will continuously reduce visibility, affect the visual range of evacuees and then affect the evacuation speed.

According to the principle of fire dynamics, the development of fire goes through three stages named accelerated combustion, stable combustion and the extinguishing stage. The spread of smoke in each stage is also different. In the stage of accelerated flame combustion, fire smoke is generated and continues to spread upwards and accumulates, reaching the ceiling and continuing to spread around. The fire has developed into a stable combustion stage, and a large amount of smoke generated before has accumulated in the ceiling and formed a stable smoke layer, which continues to settle. Until the extinguishing phase, smoke is continuously generated and fills the entire atrium. Figure 6 shows the schematic diagram of smoke spread under working Cases 1~5.

It is not difficult to see from Figure 6 that the smoke rises first under the action of thermal buoyancy, and after reaching the ceiling, it begins to spread horizontally until it fills the ceiling and spreads into the ring corridor. Due to the restrictions of the walls on the east and west sides of the atrium, the smoke begins to fill downward, and then the smoke continues to be generated. At 300 s, it has basically filled the atrium, and the smoke layer in the atrium begins to settle slowly, with a clear boundary with the cold air layer.

Comparing Cases 1, 3 and 4, we find that different heat release rates will make a significant difference in the speed of smoke spread; under the condition of a large heat release rate, the smoke spreading rate is greater than that of the small heat release rate, and the thickness of the stable smoke layer is also significantly thicker. It is not difficult to understand that the greater the heat release rate is, the more obvious the thermal buoyancy effect is, so the stronger the winding effect is. Therefore, it can reach the roof earlier, gather, and begin to settle. When the natural smoke exhaust (Cases 1, 2) and mechanical smoke exhaust (Cases 4, 5) are turned on, the concentration and thickness of the smoke layer will be significantly reduced. This is because the opening of the smoke exhaust vent makes the smoke continuously pump outside, reducing the concentration of the smoke layer and making the thickness of the smoke layer decrease. From this point of view, the smoke exhaust effect of the large atrium is good, and it is very necessary to set up a reasonable smoke exhaust system.

3.2. Vertical Smoke Temperature Distribution in Atrium

The fire produces a large amount of smoke, and releases huge heat to produce a high temperature. A high temperature environment and toxic smoke will bring difficulties to the safe evacuation of trapped people. Long-term exposure to smoke will seriously damage people's physical functions, and they may lose the ability to escape. The study of the temperature distribution law of smoke in an atrium can not only provide a reference for building fire design, but also provide guidance for personnel evacuation during a fire. Figures 7–11 are the variation charts of vertical smoke temperature in the atrium under five different working conditions, and six measurement points at different positions are selected as analysis objects in the vertical direction: V1 (17.3 m), V4 (14.3 m), V7 (11.3 m), V10 (8.3 m), V13 (5.3 m), V16 (2.3 m).

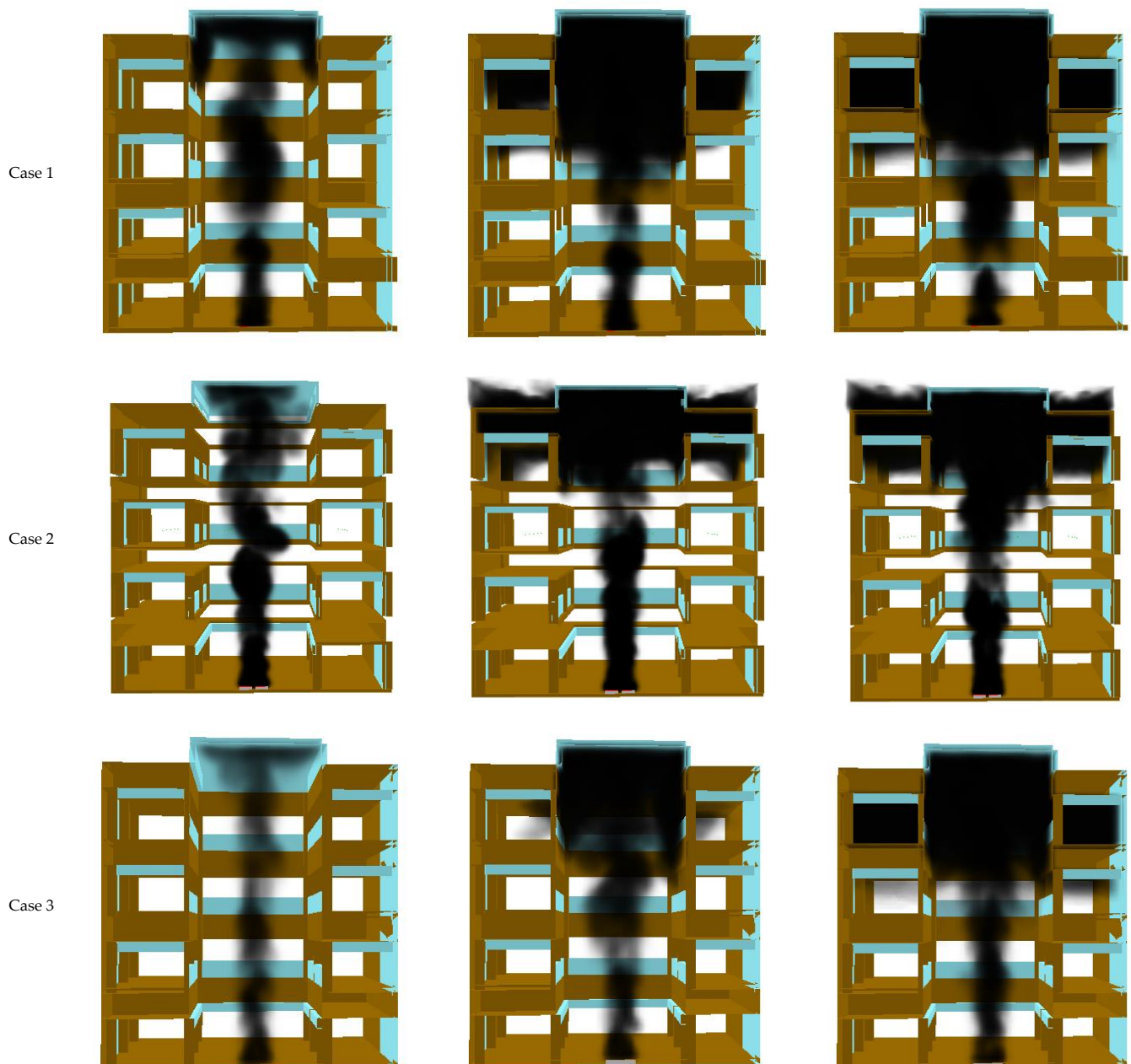


Figure 6. Cont.

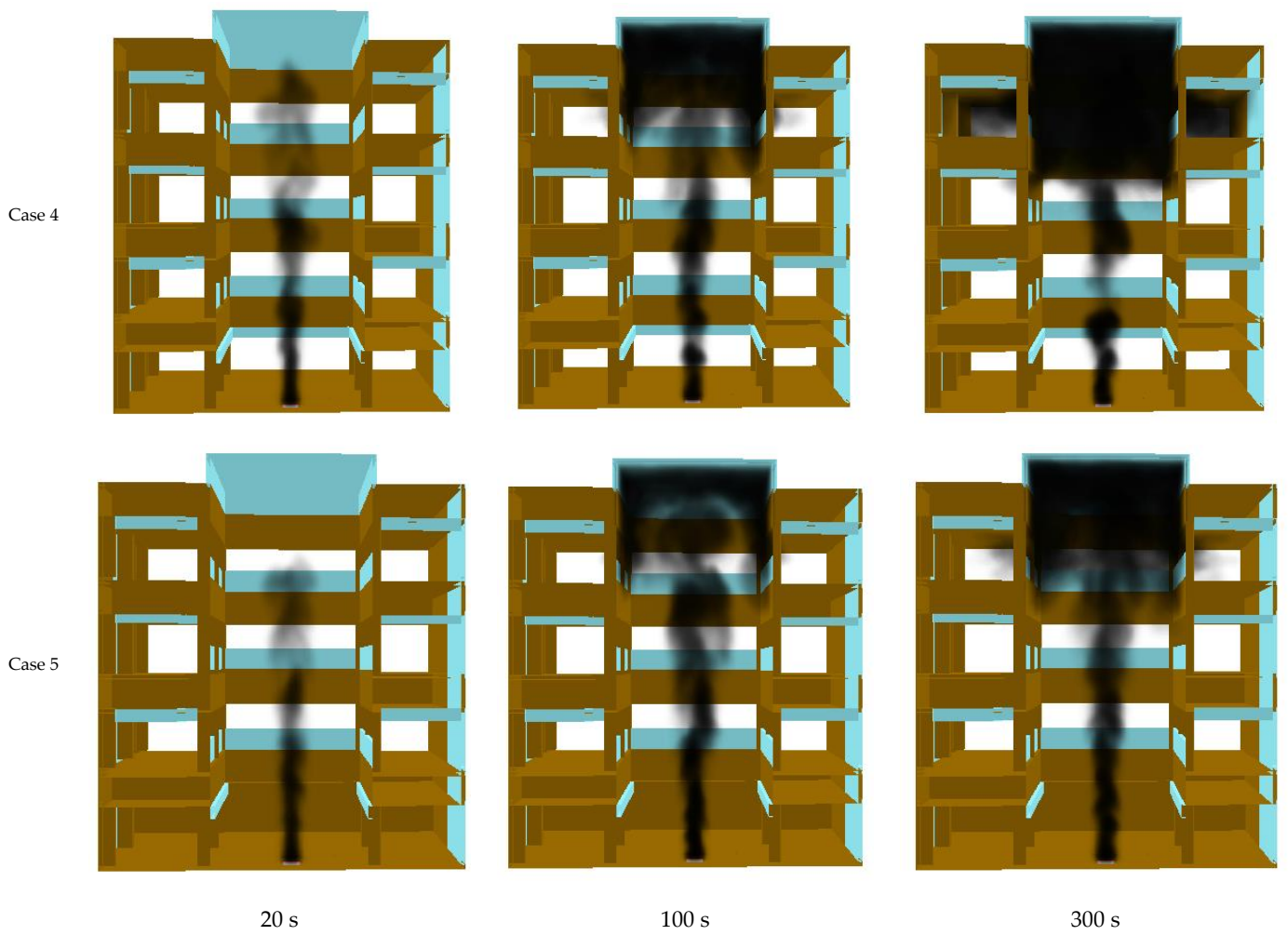


Figure 6. Comparison of smoke layer thickness at different times in Cases 1~5.

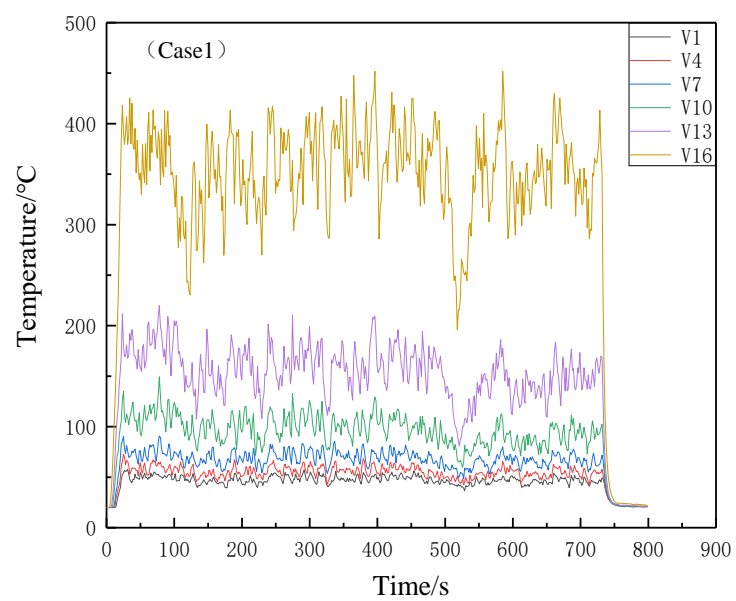


Figure 7. Temperature variation of measuring points at different heights above the atrium in Case 1.

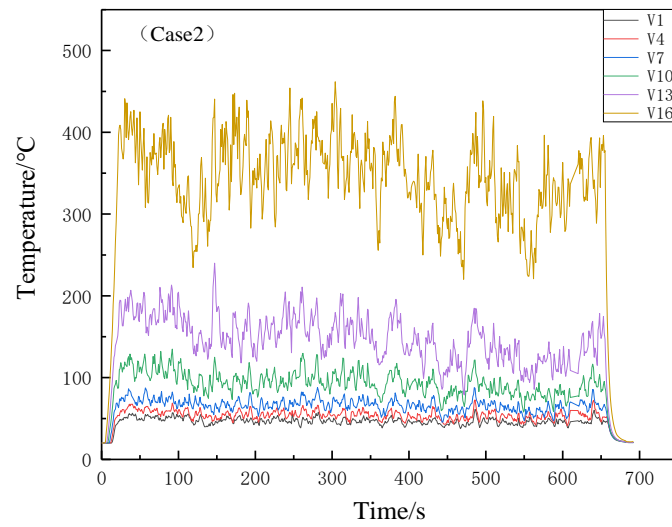


Figure 8. Temperature variation of measuring points at different heights above the atrium in Case 2.

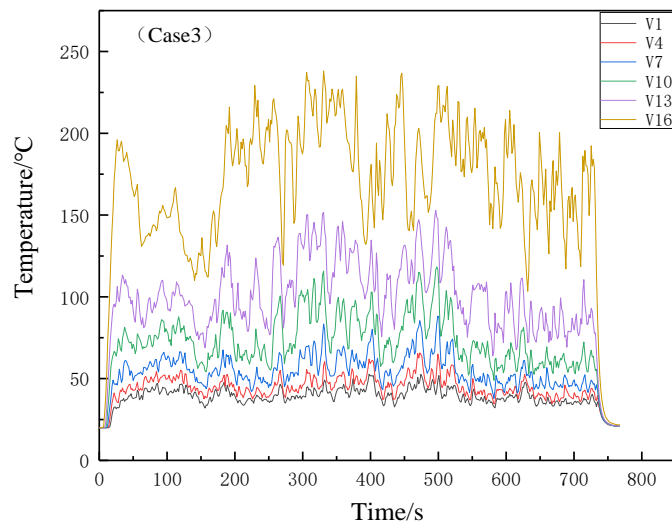


Figure 9. Temperature variation of measuring points at different heights above the atrium in Case 3.

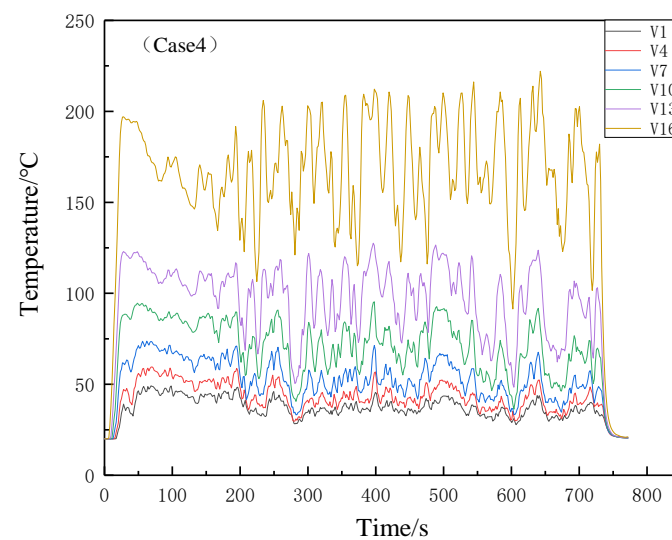


Figure 10. Temperature variation of measuring points at different heights above the atrium in Case 4.

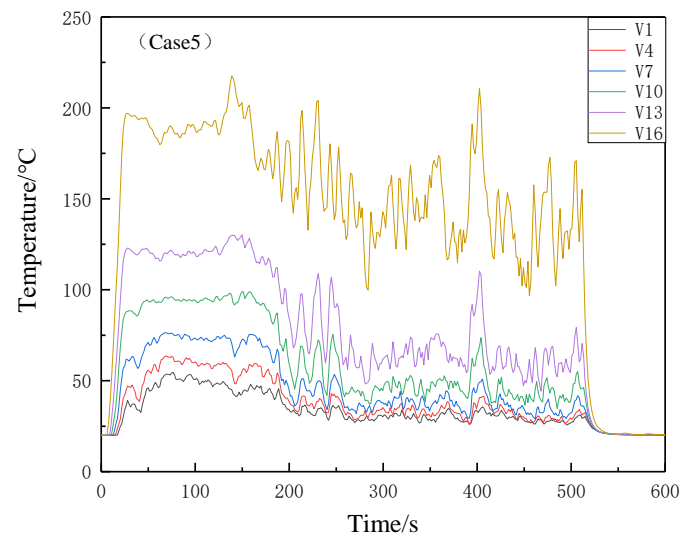


Figure 11. Temperature variation of measuring points at different heights above the atrium in Case 5.

It can be seen that the change trend of smoke temperature rise under different working conditions is basically similar. Regardless of the heat release rate and whether the smoke exhaust system is turned on, the rise of smoke temperature has successively experienced the three stages of rise, fluctuation within a certain range and decrease, which is consistent with the three stages of occurrence and development of fire explained by combustion theory. In the stable combustion stage of the ignition source, the smoke temperature will fluctuate within a certain range, and we regard it as the stable stage of the smoke temperature rise (Figures 7–11). Under different working conditions, the stabilization stage of smoke temperature rise is different, which is mainly reflected in the stable value of smoke temperature rise and the time when the stable section disappears.

When a fire starts, the heat released by the fire is limited, and the rise of smoke temperature is relatively slow. Then, the fire becomes violent, and the temperature gradient increases rapidly and it quickly reaches the maximum temperature. Comparing Figures 7, 9 and 10, it can be seen that under the same natural filling conditions, the temperature stability values of the measurement point closest to the fire source under different heat release rate in Case 1 (1.5 MW), Case 3 (0.7 MW) and Case 4 (0.34 MW) decrease sequentially. This indicates that the greater the heat release rate is, the greater the average temperature of the smoke in the atrium is. The greater the distance between the smoke and the fire source above the atrium, the lower the temperature of the smoke is; that is, the thermocouple closest to the fire source has the highest temperature and the thermocouple farthest away has the lowest temperature. As the smoke moves far away in the upper layers, heat is gradually dissipated. However, the time it takes for the smoke temperature stabilization to disappear is not much different. When the natural smoke exhaust mode (Cases 1 and 2) is turned on, it mainly has a greater impact on the smoke temperature on the upper floor of the atrium, and has little impact on the smoke temperature near the fire source. This is because the natural smoke exhaust strategy only opens the top glass window of the atrium to accelerate the flow of smoke near it, so that the heat exchange is accelerated, while the position near the fire source far from the glass window receives little impact. After turning on the mechanical smoke exhaust system (Cases 4 and 5), the temperature decreases, which also causes the temperature stability section to disappear earlier.

Figure 12 shows the change of the average temperature of the vertical smoke stabilization section of the atrium with the height of the fire source center under the conditions of Cases 1–5. It can be clearly known that the uniform temperature of the smoke stabilization section is directly related to the heat release rate of the fire. In addition, the use of natural smoke exhaust (Cases 1 and 2) or mechanical smoke exhaust (Cases 4 and 5) also has an impact on the uniform temperature of the smoke stabilization section. Turning on the

smoke exhaust system will accelerate the heat exchange between the smoke and outside, so that the smoke cooling temperature is reduced. However, from Figure 12, the magnitude of this temperature reduction is not obvious, indicating that a single smoke exhaust mode has a poor effect on the flow control of smoke.

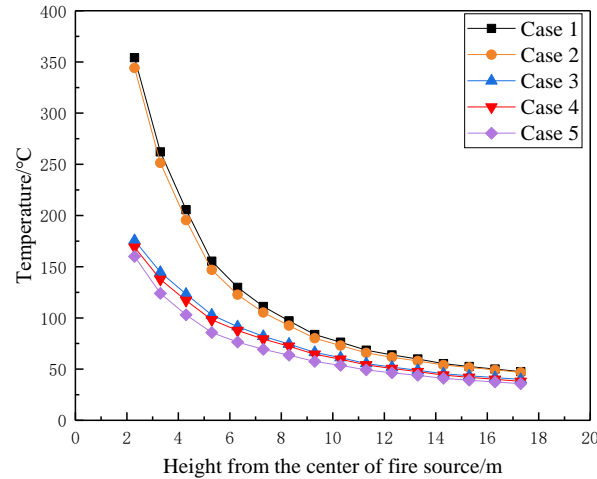


Figure 12. Variation of vertical smoke average temperature in atrium with height from fire source center in Cases 1~5.

In order to describe the distribution of vertical smoke temperature in the atrium more intuitively and accurately, we introduced the McCaffrey plume model [19]. The McCaffrey plume model is a semi-empirical formula, which is fitted by a large number of experimental results. It is applicable to the calculation of plume mass flow under the condition of both small area fires and large area fires, maintaining certain universality. It is widely used to study the flame plume in building fires [20–23]. The expression is as follows:

$$\Delta T = \left(\frac{\kappa}{0.9 \cdot \sqrt{2g}} \right)^2 \left(\frac{z}{\dot{Q}^{2/5}} \right)^{2\eta-1} \cdot T_{\infty} \tag{2}$$

where ΔT represents the difference between the temperature at appointed altitude and the ambient temperature, K; g is the acceleration of gravity, 9.81 m/s^2 ; \dot{Q} is the heat release rate of the fire, kW; z is the height, m; T_{∞} is the ambient temperature, 293 K. The three zones of the axisymmetric buoyant plume are shown in Figure 13. The values of κ and η of the McCaffrey plume model are shown in Table 3.

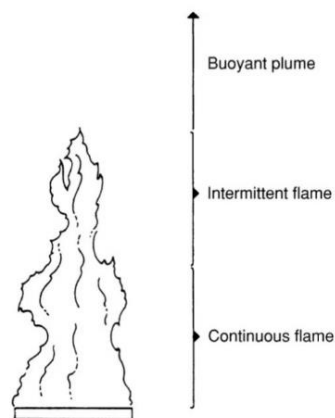


Figure 13. The three zones of the axisymmetric buoyant plume.

Table 3. Values of κ and η .

Zone	$z/\dot{Q}^{2/5}$ [m/kW ^{2/5}]	κ	η
Continuous flame zone	<0.08	6.8 [m ^{1/2} /s]	1/2
Intermittent flame zone	0.08–0.2	1.9 [m/kW ^{1/5} s]	0
Plume zone	>0.2	1.1 [m ^{4/3} /kW ^{1/3} s]	−1/3

However, considering the factors of multi-fire flame fusion, air flow and smoke exhaust system in this working condition, the McCaffrey plume model above needs to be corrected. We still use $z/\dot{Q}^{2/5}$ as the independent variable to draw the scatter diagram of smoke temperature rise changing with the vertical height and the heat release rate of the fire source, and then carry out subsection fitting correction, as shown in Figure 14.

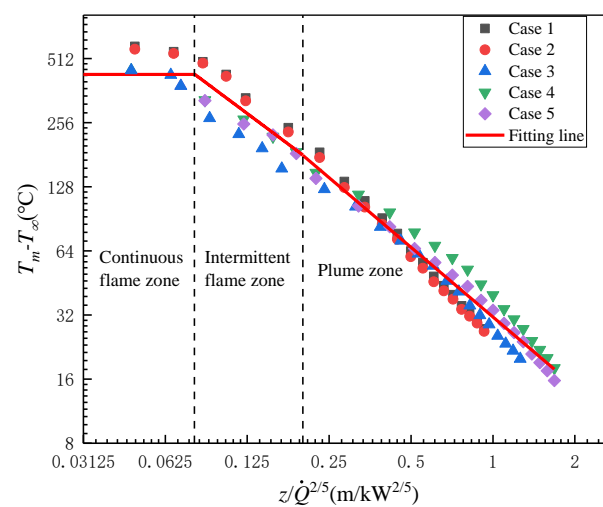


Figure 14. Variation of smoke temperature rise with $z/\dot{Q}^{2/5}$.

The modified κ and η values are shown in Table 4.

Table 4. Modified values of κ and η .

Zone	$z/\dot{Q}^{2/5}$ [m/kW ^{2/5}]	κ	η
Continuous flame zone	<0.08	4.84 [m ^{1/2} /s]	0.5
Intermittent flame zone	0.08–0.2	1.46 [m/kW ^{1/5} s]	0.03
Plume zone	>0.2	1.31 [m ^{4/3} /kW ^{1/3} s]	−0.04

3.3. Horizontal Smoke Temperature Distribution under the Ceiling of the Atrium

The temperature distribution below the atrium ceiling is similar to ceiling jet. The smoke rises from the atrium fire source to the ceiling, and then spreads around, filling the entire atrium. Under all cases, the smoke temperature reached a maximum value directly above the fire source, and decreased on the east and west sides as it moved away from the center point, showing an exponential attenuation mode. The temperature attenuation rate is not only directly related to the heat release rate, but also has a certain relationship with the smoke exhaust system. In order to analyze this attenuation relationship more intuitively and qualitatively, we make the average temperature of the smoke under the atrium ceiling dimensionless according to the following equation [24],

$$\Delta T / \Delta T_0 = e^{-\alpha x / H} \tag{3}$$

where ΔT represents the temperature of the measurement point in the 'x' direction, °C; ΔT_0 represents the temperature at the center position directly above the fire source, °C; α is the attenuation coefficient of dimensionless smoke temperature rise with dimensionless distance from fire source; x is the distance from the center point, m; H is the clear height of atrium, 19.8 m.

Figure 15 shows the variation of the horizontal dimensionless smoke temperature rise $\Delta T/\Delta T_0$ with the dimensionless distance x/H from the fire source at the height of 18.3 m below the atrium ceiling under various working conditions. The correlation coefficient of the fitting curve reaches more than 0.95 under all cases, indicating that the consistency between the data and the model was good. Table 5 shows the attenuation coefficient of dimensionless smoke temperature rise with dimensionless distance from the fire source.

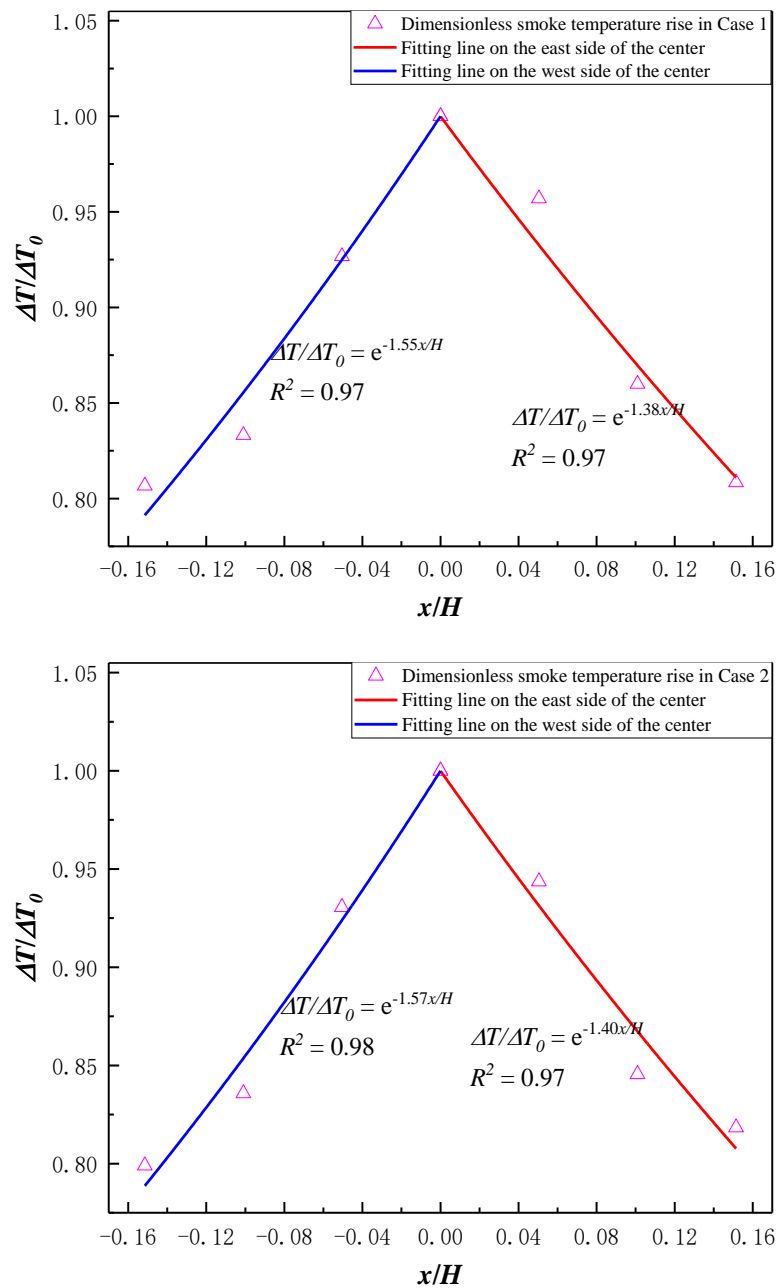


Figure 15. Cont.

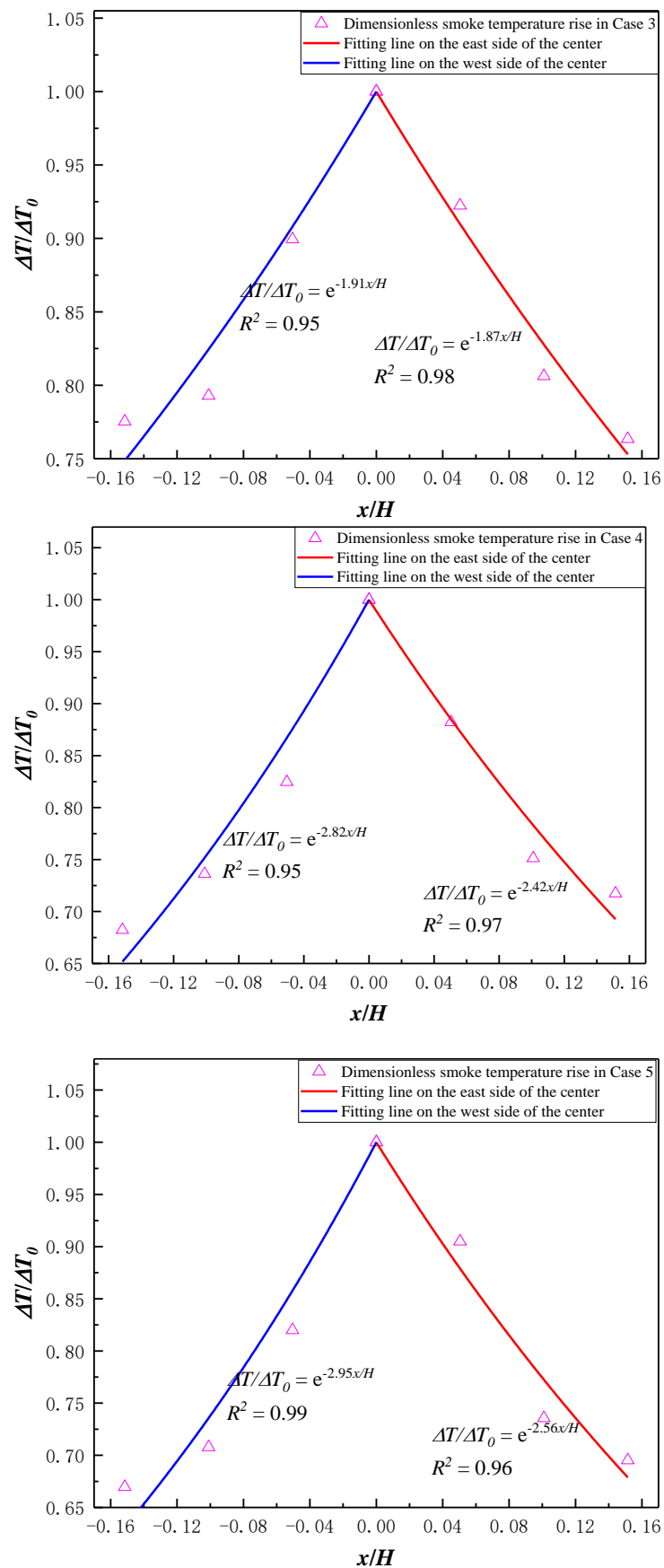


Figure 15. Variation of dimensionless smoke temperature rise $\Delta T/\Delta T_0$ under atrium ceiling with dimensionless distance from fire source x/H in Cases 1~5.

Table 5. Attenuation coefficients of dimensionless smoke temperature rise with dimensionless distance from fire source.

	Case 1	Case 2	Case 3	Case 4	Case 5
α (East)	1.38	1.40	1.87	2.42	2.56
α (West)	1.55	1.57	1.91	2.82	2.95

It can be seen from Figure 15 that the variation of lateral dimensionless smoke temperature rise under the atrium ceiling with the distance between dimensionless and fire source has a greater relationship with the heat release rate. The larger the heat release rate is, the higher the smoke temperature in the atrium is, and the greater the mass flow rate is, also the faster the smoke spreads, resulting in a smaller attenuation coefficient. The smoke temperature shows a trend of attenuation from the central position to both sides, and the left and right sides are basically symmetrically distributed, but there are still slight differences. Possibly because the east side of the building has a protruding space, as well as the obstruction of the smoke barrier, the east side of the smoke accumulates in a small area, and the heat is not dispersed, resulting in a smaller attenuation rate than the west side. Analyzing the influence of different experimental scenarios, it is found that the dimensionless temperature rise attenuation rate is also related to the use of the smoke exhaust system. Specifically, after opening the natural smoke exhaust vents (Cases 1 and 2) and turning on the mechanical smoke exhaust (Cases 4 and 5), the smoke flow is accelerated, and the heat exchange with the external environment is promoted, bringing the cooling effect to the smoke. Therefore, it will lead to the increase of the attenuation coefficient, which means that the attenuation rate also increases. Additionally, the effect of mechanical smoke exhaust is better than that of natural smoke exhaust.

4. Conclusions

In this paper, the smoke spread law and temperature distribution characteristics of large indoor pedestrian street fires are investigated using a combination of numerical simulation and full-scale experiments. The main conclusions are summarized as follows:

- (1) After a series of comparative studies, it is found that the conclusions obtained from the numerical simulation study and the full-scale experimental study are in good agreement. The smoke spread rate increases with the increase of the heat release rate of the fire source, and the thickness of the stable smoke layer increases as well. When the smoke exhaust system is turned on, the smoke volume decreases rapidly, the smoke layer thickness decreases and the visibility increases.
- (2) The higher the heat release rate of the fire source, the higher the average temperature of the smoke in the atrium. There exists an obvious stabilization phase of the smoke temperature. When the smoke exhaust system is turned on, the smoke temperature decreases and the stabilization phase of the smoke temperature is shortened. In the actual scenario, the effect of multi-system cooperative smoke exhaust is better than the smoke exhaust effect of single smoke exhaust system. The smoke temperature distribution obtained from the numerical simulation agrees well with the modified McCaffrey plume model.
- (3) The horizontal dimensionless smoke temperature rise below the atrium ceiling changes exponentially with the dimensionless distance from the fire source. The greater the heat release rate, the greater the smoke mass flow rate and smoke spread rate, and the smaller the attenuation coefficient. The attenuation coefficient increases when the smoke exhaust system is turned on. Furthermore, this indicates that the effect of mechanical smoke exhaust is better than that of natural smoke exhaust. Among the factors related to the attenuation coefficient, the effect of the heat release rate of the fire is stronger than that of smoke exhaust. In practical applications, using low calorific value materials, reducing the stacking of combustibles and adjusting the

exhaust mode and volume all contribute to the increase of the attenuation coefficient to decrease the atrium temperature as soon as possible.

Author Contributions: Conceptualization, Q.L. and Y.Z.; methodology, Y.Z.; software, Q.L. and W.L.; validation, W.L., B.C. and Y.Z.; formal analysis, Q.L.; investigation, Q.L.; resources, W.L.; data curation, B.C.; writing—original draft preparation, Q.L.; writing—review and editing, Q.L. and Y.Z.; visualization, M.Z., H.W. and J.C.; supervision, W.L. and J.C.; project administration, M.Z.; funding acquisition, B.C. and H.W. All authors have read and agreed to the published version of the manuscript.

Funding: This work was supported by the Regional Development Science and Technology Program of Fujian Province (No. 2019Y3002) and Natural Science Foundation of Hunan Province (No. 2021JJ30860).

Institutional Review Board Statement: Not applicable.

Informed Consent Statement: Not applicable.

Data Availability Statement: Not applicable.

Conflicts of Interest: The authors declare no conflict of interest.

References

- Xu, X.; Wang, Z.; Liu, X.; Ji, C.; Yu, N.; Zhu, H.; Li, J.; Wang, P. Study on Fire Smoke Control in Super-high Building Atrium. *Procedia Eng.* **2018**, *211*, 844–852. [[CrossRef](#)]
- Wang, R.; Lan, X.; Xu, L. Smoke spread process under different heights based on numerical simulation. *Case Stud. Therm. Eng.* **2020**, *21*, 100710. [[CrossRef](#)]
- Hu, L.H.; Huo, R.; Li, Y.Z.; Wang, H.B.; Chow, W.K. Full-scale burning tests on studying smoke temperature and velocity along a corridor. *Tunn. Undergr. Space Technol. Inc. Trenchless Technol. Res.* **2004**, *20*, 223–229. [[CrossRef](#)]
- Huo, R.; Li, Y.; Yu, M.; You, F.; Zhou, Y. Preliminary study on mechanical smoke exhaust in large-space building fire. *Fire Sci. Technol.* **2001**, *5*, 440–452.
- Rho, J.; Ryou, H. A numerical study of atrium fires using deterministic models. *Fire Saf. J.* **1999**, *33*, 213–229. [[CrossRef](#)]
- Mowrer, F.W. Enclosure smoke filling revisited. *Fire Saf. J.* **1999**, *33*, 93–114. [[CrossRef](#)]
- Rafinazari, A.; Hadjisophocleous, G.V. An investigation of the effect of make-up air velocity on smoke layer height with asymmetric openings and rotational air flow in atrium fires. *J. Build. Eng.* **2020**, *27*, 100933. [[CrossRef](#)]
- Long, Z.; Liu, C.; Yang, Y.; Qiu, P.; Tian, X.; Zhong, M. Full-scale experimental study on fire-induced smoke movement and control in an underground double-island subway station. *Tunn. Undergr. Space Technol.* **2020**, *103*, 103508. [[CrossRef](#)]
- Jiao, A.; Lin, W.; Cai, B.; Wang, H.; Chen, J.; Zhang, M.; Xiao, J.; Liu, Q.; Wang, F.; Fan, C. Full-scale experimental study on thermal smoke movement characteristics in an indoor pedestrian street. *Case Stud. Therm. Eng.* **2022**, *34*, 102029. [[CrossRef](#)]
- Tian, H.; Cai, W. Design of fire smoke control in commercial indoor pedestrian street. *Fire Sci. Technol.* **2013**, *32*, 1349–1351.
- Zhao, Z. *Research on Smoke Flow and Control of Fire in Indoor Pedestrian Street*; Central South University: Changsha, China, 2014.
- Jiang, C. *Numerical Simulation Study on Fire Smoke Control in Atrium Space of a Shopping Mall*; Anhui Jianzhu University: Hefei, China, 2018.
- McGrattan, K.; McDermott, R.; Weinschenk, C.; Forney, G. *Fire Dynamics Simulator Users Guide*, 6th ed.; Nist Special Publication: Washington, DC, USA, 2013.
- Lv, S. *Fire and Escape Simulation Chinese Tutorial and Engineering Application*; Beijing Chemical Industry Press: Beijing, China, 2014.
- GA/T 999-2012; Field Verification Method for Anti-Smoke System Performance Hot Smoke Test Method. Ministry of Public Security of the People's Republic of China. China Standards Press: Beijing, China.
- NIST Special Publication 1019, April 2015. Fire Dynamics Simulation (Version 6.2.0)—User's Guide*; National Institute of Standards and Technology: Gaithersburg, MD, USA, 2015.
- Dai, J. Test and Correction of Heteroscedasticity in One-Way ANOVA. *Stat. Decis.* **2017**, *8*, 23–26.
- Zhong, M.; Li, P.; Liu, T. Experimental study on fire smoke movement in a multi-floor and multi-room building. *Sci. China Ser. E Eng. Mater. Sci.* **2005**, *48*, 292–304. [[CrossRef](#)]
- Karlsson, B.; Quintiere, J.G. *Enclosure Fire Dynamics*; CRC Press: Boca Raton, FL, USA, 1999.
- Walter, W.J.; Glenn, P.F. *NISTTN1431, A Technical Reference for CFAST: An Engineering Tool for Estimating Fire and Smoke Transport*; National Institute of Standards and Technology, Building and Fire Research Laboratory: Gaithersburg, MD, USA, 2000; pp. 17–77.
- Cheng, Y.; Chen, L.; Zhang, M. The Analysis and Estimation of the Plume Models in the Development Fires. *Fire Saf. Sci.* **2002**, *11*, 132–136.
- Han, R.; Zhu, G.; Zhang, G.; Zhang, Y. Optimization Design of Smoke Extraction in the High-rise Building Wit Atrium. *Ind. Saf. Environ. Prot.* **2013**, *39*, 48–51.

23. Tao, Y.; Lu, K.; Chen, X.; Mao, S.; Ding, Y.; Zhao, Y. Experimental investigation on the temperature profile of large scale RP-5 aviation kerosene pool fire in an open space. *Fuel* **2020**, *264*, 116852. [[CrossRef](#)]
24. Gong, L.; Jiang, L.; Li, S.; Shen, N.; Zhang, Y.; Sun, J. Theoretical and experimental study on longitudinal smoke temperature distribution in tunnel fires. *Int. J. Therm. Sci.* **2016**, *102*, 319–328. [[CrossRef](#)]

Disclaimer/Publisher's Note: The statements, opinions and data contained in all publications are solely those of the individual author(s) and contributor(s) and not of MDPI and/or the editor(s). MDPI and/or the editor(s) disclaim responsibility for any injury to people or property resulting from any ideas, methods, instructions or products referred to in the content.